Journal of the Korean Vacuum Society
Vol. 3, No. 2, June 1994, pp. 158-165

〈연구논문〉

Electrohydrodynamic Treatment of the Shape and Stability of Liquid Metal Ion Sources

Moon Sung Chung, Jeom Soo Choi and Ji Mo Park

Department of Physics, University of Ulsan, Ulsan 680-749, Korea
(Received March 25, 1994)

액체금속 이온 소오스의 모양과 안정도에 대한 전자유체역학적 연구

정문성 · 최점수 · 박지모

울산대학교 자연과학대학 물리학과
(1994년 3월 25일 접수)

Abstract — An improved conical model is presented for the shape of a liquid metal ion source. In this model, we use the Taylor cone of the conducting fluid as the zeroth-order configuration and treat electrohydrodynamically the first-order contribution of its surface deformation. A set of first-order electrohydrodynamic equations of the fluid are analytically solved by assuming that the apex protrusion h due to the applied electric stress is associated only with the change in the apex region of $r<a$. Here, a is a parametric constant. This assumption leads to take the angular deformation $\zeta=(r/a)^s\varepsilon(t)$ for $r<a$ and $(a/r)\varepsilon$ for $r>a$, where the exponent s is a quantity associated with the evolved shape. The use of ζ in the set of equations makes the breakdown voltage of the surface have the form $V_C(r, h)=V_0(h)+V_1(r, h)$ when the fluid has the protrusion h at the apex. Here, $V_0(h)$ is the voltage needed for sustaining the zeroth-order shape of the fluid surface and $V_1(r, h)$ is the additional voltage for the onset of instability which is the ion emission from the apex. The obtained critical voltage V_C is found to be in reasonable agreement with experiments and, more importantly, explains the local instability which is physically required. It is physically argued that for $V>V_C$, $\zeta>0$ and $0<s\leq 0.2$. This implies that the conducting fluid changes from the Taylor cone to a cusp near the onset of instability.

요 약 — 액체금속 이온 소오스의 모양에 대한 개선된 원추 모델을 제시하였다. 이 모델에서는 전도성 유체의 테일러 원추를 0차 모양으로 하고 원추에서 벗어난 변형을 전자유체 역학적으로 취급하였다. 외부의 전기적 스트레스 때문에 원추정점에서 일어나는 돌출을 오직 $r<a$의 영역에서 모양변형에만 관계하는 것으로 가정하여 일차 전자유체 역학적 방정식을 풀 수 있었다. 여기서 a는 $r>a$인 영역에서는 변형이 없다는 것으로 정의되는 값이다. 이 가정에 의하여 각변형 ζ는 다음 같은 형태를 가졌다: $r<a$인 경우는 $\zeta=(r/a)^s\varepsilon(t)$이고 $r>a$인 경우는 $\zeta=(a/r)\varepsilon$이다. 여기서 지수 s는 변형의 모양을 나타내는 값이다. 이것을 모양 방정식에 대입하여 계산한 결과 모양의 불안정되는 전위값 V_C은 위치 r과 돌출길이 h의 함수로 주어지고 또 다음과 같은 두 개의 합으로 표현할 수 있었다: $V_C(r, h)=V_0(h)+V_1(r, h)$. 여기서, V_0는 돌출이 있는 변형된 유체모양에서 0차 모양을 유지하는데 필요한 전위이고 V_1은 1차의 표면이 불안정되는 전위값으로 이온방출을 일어나는데 필요한 여분 값이다. 이렇게 얻어진 이온방출의 임계 전위 V_C는 실험치와 부합되는 값이었다. 더욱 중요한 것은 위의 V_C 형태가 국지 불안정을 설명하여 주었다. 또한 외부에서 걸어준 전위가 임계전위값을 넘을 때 각변형 $\zeta>0$이고 $0<s<0.2$인 것을 알 수 있었다. 이것은 불안정되는 근처에서는 전도성 유체의 모양이 테일러 원추에서 커습으로 바뀜을 의미한다.

This paper was supported in part by NON DIRECTED RESEARCH FUND, Korea Research Foundation, 1992.

1. Introduction

Stability of an electrically stressed conducting fluid has been studied for more than a century since Lord Rayleigh's work [1]. This subject has relevance to (i) the mechanism responsible for the formation of thunderstorms [2], (ii) the measurement of the size and density distribution of atmospheric droplets[3], (iii) the description of self-gravitating viscous liquid which can serve as a first approximation to the model of an oscillating star [4], and (iv) other applications [5]. Recently, the role of stability has been stressed in the study of operation of technological devices such as electrohydrodynamic ion sources [6-8], i.e., the liquid metal ion sources (LMIS). Even though Taylor [9] made a great success in explaining the shape and stability of the conducting fluid, the dynamics of LMIS is not satisfactorily described using a stationary Taylor cone model [10, 11]. A more rigorous and hydrodynamic approach is required [12-15].

In the current work, we treat electrohydrodynamically the shape and instability of the LMIS. We extend our model of LMIS presented in previous works [15-17] by making a more exact mathematical treatment of the evolution of the shape. The Taylor cone is used as the basis (i.e. the zeroth-order shape) and then we introduce a first-order shape correction to describe a change of the fluid surface. As a more realistic form of the surface deformation in the current work, we take $\zeta=(a/r)\varepsilon$ for $r>a$, where ζ is the angular deviation of the surface from the Taylor cone and ε is the maximum value of ζ at $r=a$. This form of ζ satisfies the condition that $r\,\zeta$ is finite as r approaches infinity, which is the case. In the previous work, we took $\zeta=(a/r)^{0.5}$ ε for $r>a$ which leads to the divergence of $r\,\zeta$ as r approaches to infinity. To solve the Laplace equations for electric and velocity potentials, Φ and Ω we use the same scheme as in the previous work [15-17]. Since the Laplace equation is unsolvable for arbitrary boundaries such as the fluid surface, we make an contribution order-analysis of Φ and Ω Then electrohydrodynamic analysis of the first-order shape leads to understanding of instability of the fluid shape.

We explain the current model and derive a set of electrohydrodynamic equations to be satisfied by the electrified conducting fluid in section 2. In section 3, we find the first-order solutions of the obtained shape equations and discuss the instability of the electrified fluid surface. Conclusions are made in section 4.

2. Conical Fluid Surface Model

An electrically stressed conducting fluid has the shape of the Taylor cone at a certain applied voltage for a sophisticated counter-electrode [9]. As the voltage increases, the fluid deforms its shape and eventually evolves to breakdown of the fluid surface. The evolution of the shape can results in a protrusion around the cone apex. Thus we use the Taylor cone as the basis and introduce a change described by an angular deformation ζ (refer to Fig. 1).

In order to describe the free fluid surface, we define the shape function F by

$$F(r,\ \theta,\ t)=\theta_0+\zeta(r,\ t)-\theta. \tag{1}$$

where $\theta_0=130.7°$ and $\theta=\theta_0$ represents the Taylor cone as shown by the dotted cone in Fig. 1. Then the evolving shape of the fluid is specified by $F=0$.

For a charged or electrically stressed surface, its equilibrium is given by the Laplace-Young equation

$$\Delta P+\frac{(\nabla\Phi)^2}{8\pi}-\gamma\left(\frac{1}{R_1}+\frac{1}{R_2}\right)=0, \tag{2}$$

where ΔP is the pressure difference across the interface, Φ the electric potential, γ the surface tension of the fluid, and R_1 and R_2 are the principal radii. To apply the Laplace-Young stress condition for finding the stable shape of the fluid, we will obtain analytic forms of ΔP, Φ and $1/R_1+1/R_2$.

When a voltage V is applied between the conducting fluid and counter-electrode, the potential Φ satisfies the following two boundary conditions

$$\Phi=V \text{ at } \theta=\theta_0+\zeta \quad \textit{(on the fluid surface)} \tag{3}$$

$$\Phi=0 \text{ at } r=r_0[P_{1/2}(\cos\theta)]^{-2} \quad \textit{(on the counter-electrode)}, \tag{4}$$

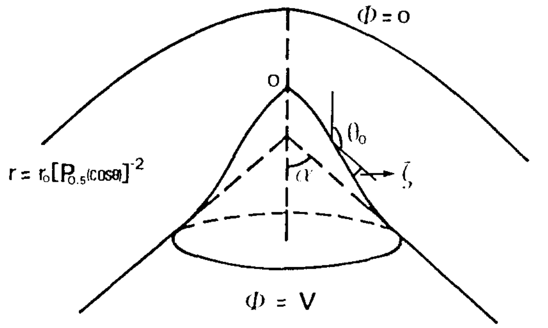

Fig. 1. Conical fluid surface model. The fluid surface is given by $\theta=\theta_0+\zeta(r)$, where $\theta_0=130.7°$ refers to the zeroth-order surface and $\zeta(r)$ is the angular deformation at position r. The dotted line is the Taylor cone of half cone angle α where $\alpha=\pi-\theta_0$. The ζ results from the spatial evolution of the apex region and the shape change in the region of $r<a$, where a is defined such that there is no change in shape for $r>a$.

where r_0 is the axial distance between the cone apex and the counter-electrode and $P_{1/2}(\cos\theta)$ is the Legendre function of degree 1/2 (refer to Fig. 1).

To obtain the hydrodynamic pressure ΔP, we consider fluid flow. It is convenient to treat the velocity potential Ω defined such that the fluid velocity $U=-\nabla\Omega$. The potential Ω satisfies the two boundary conditions

$$\frac{dF}{dt}=\frac{\partial F}{dt}-\nabla\Omega\cdot\nabla F=0$$
$$\text{at } \theta=\theta_0+\zeta \ (\textit{on the fluid surface}) \quad (5)$$

$$\boldsymbol{n}\cdot\nabla\Omega\doteq 0 \qquad \text{at } \theta=\pi \ (\textit{along the z-axis}), \quad (6)$$

where $\boldsymbol{n}$ is a unit vector normal to the fluid surface and is defined by

$$\boldsymbol{n}=\frac{\nabla F}{|\nabla F|}. \quad (7)$$

Equation (5) follows from the fact that the fluid surface is specified by $F=0$. Equation (6) expresses the condition that along the z-axis, the fluid velocity has only a vertical component. Then the hydrodynamic pressure P is obtained from the following form of Bernoulli's equation

$$-\rho\frac{\partial\Omega}{\partial t}+\frac{1}{2}\rho(\nabla\Omega)^2+P=constant. \quad (8)$$

where ρ is the mass density of the fluid. The second term in Eq. (8) is quadratic and is neglected in the current work.

From Eqs. (1) and (7), the curvature of the free fluid surface is written as

$$\left(\frac{1}{R_1}+\frac{1}{R_2}\right)=\nabla\cdot\boldsymbol{n}$$
$$=-\frac{1}{r\tan\theta}\frac{1}{\sqrt{1+r^2(\partial\zeta/\partial r)^2}}+\frac{1}{r^2}\frac{\partial}{\partial r}\left(\frac{r^3\,\partial\zeta/\partial r}{\sqrt{1+r^2(\partial\zeta/\partial r)^2}}\right). \quad (9)$$

Since the fluid surface is not a coordinate surface, the boundary conditions imposed on it cannot be directly applied. However, we can reduce them to useful forms by making the Taylor expansion of Φ and Ω about $\theta=\theta_0$. In this case, each potential is given as a sum of contributions of all-order with respect to ζ. Keeping terms up to the first-order, we will obtain a set of equations of the first-order [17].

By making the Taylor expansion of $\Phi(\theta=\theta_0+\zeta)$ about $\theta=\theta_0$, Eq. (3) is written as

$$\Phi(\theta_0+\zeta)=\Phi(\theta_0)+\zeta\left(\frac{\partial\Phi}{\partial\theta}\right)_{\theta_0}+\cdots=V. \quad (10)$$

The Φ is given as a sum of all-order contributions:

$$\Phi=\Phi_0+\Phi_1+\cdots$$

We substitute this into Eq. (10) and set the same-order term on both sides to be equal. Then the boundary conditions of the zeroth- and first-order Φ are

$$\Phi_0(\theta_0)=V, \quad (11)$$

$$\Phi_1(\theta_0)=-\zeta\left(\frac{\partial\Phi_0}{\partial\theta}\right)_{\theta_0}, \quad (12)$$

where the subscript number represents the order of contributions.

Similarly, the Taylor expansion of $\Omega(\theta=\theta_0+\zeta)$ in Eqs. (5) and (8) yields two first-order relations associated with Ω:

$$\left(\frac{\partial\Omega_1}{\partial\theta}\right)_{\theta_0}=-r^2\frac{\partial\zeta}{\partial t}, \quad (13)$$

$$\Delta P_1=\rho\left(\frac{\partial\Omega_1}{\partial t}\right)_{\theta_0}. \quad (14)$$

Here, the zeroth-order velocity potential Ω_0 is zero. This imply that no flow is allowed in the zeroth-order analysis as in the static analysis.

The curvature given by Eq. (9) is also expanded up to the first-order as follows.

$$\frac{1}{R_2}+\frac{1}{R_2}=\frac{1}{r\tan\alpha}+\frac{\zeta}{r\sin^2\theta_0}+\frac{1}{r^2}\frac{\partial}{\partial r}\left(r^3\frac{\partial\zeta}{\partial r}\right)+\cdots \tag{15}$$

Thus, we obtain the zeroth- and first-order curvatures

$$\left(\frac{1}{R_2}+\frac{1}{R_2}\right)_0=\frac{1}{r\tan\alpha}, \tag{16}$$

$$\left(\frac{1}{R_1}+\frac{1}{R_2}\right)_0=\frac{\zeta}{r\sin^2\alpha}+\frac{1}{r^2}\frac{\partial}{\partial r}\left(r^3\frac{\partial\zeta}{\partial r}\right) \tag{17}$$

where $\alpha=\pi-\theta_0$, the half angle of the Taylor cone apex.

As done in the previous work [15-17], the zeroth-order analysis can be easily made by using Eqs. (2), (4), (11), and (16). As a stress-balanced shape, the so-called Taylor cone given by $\theta=\theta_0(=130.7°)$ is obtained at a certain voltage V_T. The expressions for Φ_0 and V_T are

$$\Phi_0(r,\theta)=V\left[1-(r/r_0)^{0.5}P_{0.5}(\cos\theta)\right]. \tag{18}$$

$$V_T=\frac{4\sin\theta_0}{P_{0.5}(\cos\theta_0)}\sqrt{2\pi r_0\gamma\cot\alpha} \tag{19}$$

This is the same as obtained by Taylor [9]. It is important to note that the Taylor cone does not, by itself, imply instability of the fluid at the apex. The reason is that the stress balance designated by $\Delta P=0$ is satisfied across the entire surface of the cone, whereas the instability is a localized rather than a global phenomenon. Furthermore, V_T is not the breakdown voltage initiating the onset of instability but is the voltage sustaining the Taylor cone, i.e. the zeroth-order shape when the fluid has no protrusion from the apex. To describe the local instability, we should obtain the breakdown voltage as a function of r. It follows that the fluid shape is different from the Taylor cone. The desirable results for the realistic shape should be obtained by taking into account the first-order correction in a set of the shape equations.

3. Solutions of The First-Order Electrohydrodynamic Equations

In the previous section, we obtain a set of equations for the first-order analysis. They are the first-order boundary conditions given by Eqs. (12)-(14), the fixed boundary conditions given by Eqs. (4) and (6), the first-order curvature given by Eq. (17), and the Laplace-Young equation for the first-order surface. In solving these equations, we find deformation ζ, electric potential Φ, and velocity potential Ω self-consistently. In general, an exact treatment is impossible. However, we can make reasonable approximations to find ζ, Φ, and Ω.

We assume that a protrusion around the apex is only due to the change of the region of $r<a$, where a is a quantity dividing dynamic and static regions. This implies that the evolved shape begins to coincide the basis shape at $r=a$. Then the angular deformation ζ has the following asymptotic form

$$\zeta\rightarrow h\ \sin\alpha/r \text{ as } r\rightarrow\infty,$$

where h is the protrusion length. The r-dependence of the limiting form of ζ is found to be realistic since $r\,\zeta$ approaches a finite value. Equations. (13) and (17) also imply that ζ should be written as a function of r. A finite value of ζ at $r=0$ (i.e. at the cone apex) is found to lead to a divergent Φ and then ζ should be zero at $r=0$. Thus, we let

$$\zeta=\begin{cases}\zeta^<=(r/a)^s\ \varepsilon(t) & \text{for } r<a\\ \zeta^>=(a/r)\ \varepsilon & \text{for } r>a,\end{cases} \tag{20}$$

where the exponent s is positive and will be determined later. This is shown in Fig. 2. The deformation $\zeta^<$ has time-dependence $\varepsilon(t)$ during the evolution process while $\zeta^>$ does not at all (refer to Fig. 3). The deformation is zero at $r=0$, which is required as mentioned above. It is to note that the current formof $\zeta^>$ is different from that used in the previous work [16, 17]

Substituting Eq. (20) into Eq. (12), we obtain the first-order boundary conditions for $\Phi^<$ and $\Phi^>$. The solution Φ which satisfies the Laplace equation ∇^2

$\Phi=0$ and the associated boundary conditions is

$$\Phi_1= \begin{cases} \Phi^<(r,\ \theta,\ t)=-V\dfrac{P_{-0.5}(\cos\theta_0)}{2\ \sin\theta_0}(a/r_0)^{0.5}\ \varepsilon(t) \\ \quad \Big[(r/a)^{s+0.5}\dfrac{P_{s+0.5}(\cos\theta)}{P_{s+0.5}(\cos\theta_0)} \\ \quad +\sum B_n(r/r_0)^{\nu_n}P_{\nu_n}(\cos\theta)\Big], \\ \Phi^>(r,\ \theta)=-V\dfrac{P_{-0.5}(\cos\theta_0)}{2\sin\theta_0}(a/r_0)^{0.5} \\ \quad \varepsilon(a/r)^{0.5}\dfrac{P_{-0.5}(\cos\theta)}{P_{-0.5}(\cos\theta_0)}, \end{cases} \tag{21}$$

where $P_\nu(\cos\theta)=0$ and $\nu_0=0.5$, $\nu_1=1.9$, $\nu_2=3.4$, etc. The superscripts $>$ and $<$ represent the regions of $r>a$ and $r<a$, respectively. Hereafter, we omit the subscript "1" for convenience when the superscript $>$ or $<$ are used. The B_n's are determined from the continuity of the potential and its derivative at $r=a$. The $n=1$ and higher terms in $\Phi^<$ make negligible contributions in the region of interest (i. e., the small r-region) and will be omitted afterwards.

Similarly, substituting Eq. (20) into Eq. (13) yields the first-order boundary conditions for $\Omega^>$ and $\Omega^<$. Thus the potential Ω which satisfies the Laplace equation $\nabla^2\Omega=0$ and the associated boundary conditions is

$$\Omega_1= \begin{cases} \Omega^<(r,\theta,t)=-a^2\dfrac{\partial\varepsilon}{\partial t} \\ \quad \Big[(r/a)^{2+s}\dfrac{P_{2+s}(-\cos\theta)}{(\partial P_{2+s}(-\cos\theta)/\partial\theta)_{\theta_0}} \\ \quad +\sum C_n(r/a)^{\mu_n}P_{\mu_n}(-\cos\theta)\Big], \\ \Omega^>=0 \end{cases} \tag{22}$$

where $[\partial P_\mu(\cos\theta)\partial\theta]_\theta=0$ and $\mu_0=4.0$. The negative sign in the argument of the Legendre function is chosen so that $\Omega^<$ satisfies the boundary condition givenby Eq. (6). Since even the leading term in the summation in $\Phi^<$ is negligible compared to the first term in the square bracket, we omit all terms in the summation.

Since fluid flow is allowed around the apex, we calculate ΔP_1 for $r<a$. Substituting Eq. (22) into Eq. (14) for ΔP_1, we obtain the first-order hydrodynamic pressure

$$\Delta P_1=\rho\Big(\frac{\partial\Omega^<}{\partial t}\Big)$$
$$=-\rho a^2(r/a)^{2+s}\frac{P_{2+s}(-\cos\theta)}{[\partial P_{2+s}(-\cos\theta)/\partial\theta]_{\theta_0}}\Big(\frac{\partial^2\varepsilon(t)}{\partial t^2}\Big) \tag{23}$$

The first-order stress balance is obtained by collecting the first-order contribution terms from the Laplace-Young equation given by Eq. (2):

$$\Delta P_1+\Big[\frac{(\nabla\Phi)^2}{8\pi}\Big]_1-\gamma\Big(\frac{1}{R_1}+\frac{1}{R_2}\Big)_1=0, \tag{24}$$

where ΔP_1 is given by Eq. (23), $(1/R_1+1/R_2)_1$ is obtained from Eqs. (17) and (20), and the first-order electric stress is

$$\Big[\frac{(\nabla\Phi)^2}{8\pi}\Big]_1=\frac{1}{4\pi r^2}\Big[\frac{\partial\Phi_0}{\partial\theta}\frac{\partial\Phi_1}{\partial\theta}+\zeta\frac{\partial\Phi_0}{\partial\theta}\frac{\partial^2\Phi_0}{\partial\theta^2}\Big]_{\theta_0}, \tag{25}$$

where ζ is given by Eq. (20), Φ_0 given by Eq. (18), and Φ_1 given by Eq. (21).

We assume the harmonic time-dependence of $\varepsilon(t)$: $\varepsilon(t)=\varepsilon e^{-i\omega t}$. The fluid undergoes the dynamical instability as ω^2 becomes negative. Thus the instability condition is $\omega^2=0$. Since $\Delta P_1=\omega^2\times$[a factor] as given by Eq. (23), the instability condition is $\Delta P_1=0$. When $\Delta P_1=0$, Eq. (24) yields

$$V=V_1(r,h)$$
$$=\frac{4\ \sin\theta_0}{P_{-0.5}(\cos\theta_0)}\sqrt{\pi(r_0-h)\gamma\frac{\sin^{-2}\alpha+s(2+s)}{D_1(a/r)^s-D_2}}, \tag{26}$$

where

$$D_1=\frac{0.5+s}{\sin\alpha}\frac{P_{-0.5+s}(\cos\theta_0)}{-P_{0.5+s}(\cos\theta_0)}-(1+s)\ \cot\alpha, \tag{27}$$

$$D_2=\frac{0.5+s}{\sin\alpha}\frac{P_{-0.5+s}(\cos\theta_0)}{-P_{0.5+s}(\cos\theta_0)}-(1.5+s)\ \cot\alpha, \tag{28}$$

In Eq. (26), we replace r_0 by r_0-h to take into account the effect of the apex protrusion. The voltage $V_1(r,\ h)$ is the additional voltage required for the onset of instability at the position r distant from the apex. Therefore, when the fluid has a protrusion h, the critical voltage V_C for the onset of instability is givenby [17]:

$$V_C(r,\ h)=V_0(h)+V_1(r,\ h), \tag{29}$$

where V_0 is the voltage needed for sustaining the zeroth-order shape. It is clear that V_0 is not V_T which is the voltage for formation of the Taylor cone. That is, V_T and V_0 are the voltages for the zeroth-order shape before and after evolution from the Taylor cone, respectively. Then V_0 is obtained by replacing r_0 by r_0-h in the form of V_T given by Eq. (19).

Since V_1 changes with position r, V_C explains the local instability. This result is much different from Taylor's or other static results. Chung *et al.* [17] have already obtained the same form of V_C given by Eq. (29). However, both ζ and V_1 obtained in the current work are different from those obtained in the previous work. It is found that the current result is more realistic and more physically meaningful.

The problem in the current model is that quantities a and s are not uniquely determined. Unfortunately, complications get worse because a and s are intercorrelated. The parametric constant a is defined so that the fluid surface has no change for $r>a$. The a is used as a boundary value in dividing the whole region into the inside region of $r<a$ and the outside region of $r>a$. Thus the best choice of a can be made so that the two set of electric potentials $\Phi^<$ and $\Phi^>$ and velocity potentials $\Omega^<$ and $\Omega^>$ can be matched most smoothly. Instead of such a numerical work, we use the geometric relation between a and h and choose an appropriate value of a/h. From the geometry shown in Fig. 1, we the following relation

$$a/h=\sin\alpha/\varepsilon \qquad (30)$$

In calculation of V_C, we choose $a/h=2$, i.e. $\varepsilon=0.38$. This implies that the region undergoing change is two times as large as protrusion.

The quantity s represents the curvature of the evolved shape as in Eq. (20) (refer to Fig. 2). Even though we cannot calculate s directly, we obtain the range of s by two physical requirements. First, it is physically required that V_C increases with increasing r. That is, D_1 given by Eq. (27) is positive. It follows that

$$0<s\leq 0.6 \qquad (31)$$

Secondly, it is also physically required that the ra-

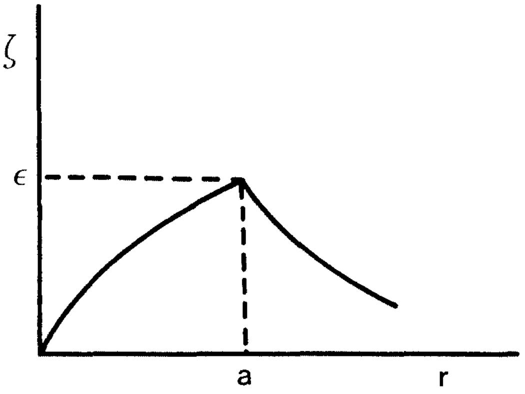

Fig. 2. Angular deformation ζ. The ζ is given Eq. (20) in the text. It has the maximum value ε at $r=a$ and has the limiting value of h $\sin\alpha/r$ as $r\to$ large.

dial velocity $U_r=-\partial\Omega^</\partial r$ is negative for $r<a$. This is the relative velocity with respect to the velocity ofthe apex, i.e., the origin of the coordinates. By Eq. (22), this requirement reduces the inequality

$$0<s\leq 0.2 \qquad (31)$$

We examined the fluid shape for $s=0.1$ and $s=0.2$ using the numerical table of Legendre functions [18]. It is found that either choice of $s=0.1$ or $s=0.2$ yields almost the same value of V_C in the region of interest. Therefore, we take $s=0.2$ in obtaining the numerical values of $V_C(r)$ as shown in Table 1. For the present, we can not determine the exact value of s. This reflects the fact that in general, the Laplace equation cannot be analytically solved for an arbitrary geometry, i.e. a free fluid shape. Through the numerical calculations over the entire range $0<s\leq 0.2$, we can find the most appropriate value of s, which is not done in the current work.

Now we discuss the property of the time-dependence term $\varepsilon(t)$. By the Laplace-Young equation given by Eq. (24), ΔP_1 is positive for $V<V_1$ and negativefor $V>V_1$. This implies that by Eq. (23), $\partial^2\varepsilon/\partial t^2$ is negative for $V<V_1$ and positive for $V>V_1$. The term $P_{2+s}(-\cos\theta)/[\partial P_{2+s}(=\cos\theta)/]_\theta$ in Eq. (23) is positive for $0<s\leq 0.2$. During the period that the applied voltage V goes from the Taylor voltage V_T to the critical voltage V_C, $\partial^2\varepsilon/\partial t^2$ is positive. Since $\varepsilon(t)=0$ at $t=0$ when the Taylor cone is formed, $\varepsilon(t)$

Table 1. Critical voltage for breakdown of the surface of liquid Ga, $V_C(r, h)$. Here, r is the distance from the cone apex and h is the protrusion length of the apex. In the calculations of V_1 and V_C given by Eqs. (26) and (29), we choose $r_0=2$ mm and $a=2h$ (i.e. $\varepsilon=0.38$), where r_0 is the axial distance between the Taylor cone apex and the counter-electrode and the parameter a is defined such that there is no shape change for $r>a$. The values of V_C at $r=0$ represent the voltages for ion emission from the apex

	h (mm)	r (μm)	V_1 (kV)	V_C (kV)
Current work	0.0	all	0.0	overall equil.
	0.1	0.0	0.0	16.7
		0.1	5.8	22.5
		1.0	7.8	24.5
	0.5	0.0	0.0	14.8
		0.1	4.3	19.1
		1.0	5.6	20.4
	1.0	0.0	0.0	12.1
		0.1	3.3	15.4
		1.0	4.2	19.0
	1.5	0.0	0.0	8.6
		0.1	2.2	10.8
		1.0	2.8	11.4
Taylor's formula [9]		all		17.1
Experiments [7, 19-21]		≈ 0		5-10

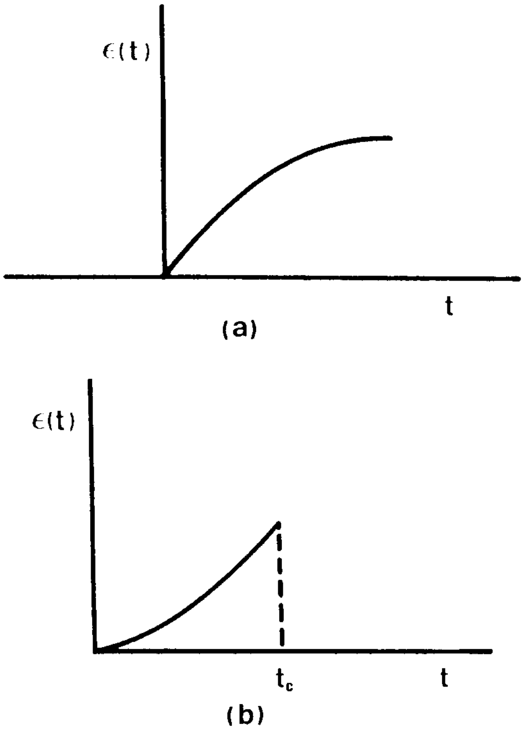

Fig. 3. Time-Dependence of deformation, $\varepsilon(t)$. Since ΔP_I is positive for $V<V_1$ and negative for $V>V_1$, $\partial^2\varepsilon/\partial t^2$ is negative for $V<V_1$ and positive for $V>V_1$. Thus, for $V<V_C$ (a), $\varepsilon(t)\to\varepsilon_0$ as $t\to\infty$: The fluid surface is stable. For $V>V_C$ (b), $\varepsilon(t)\to\infty$ as $t\to\infty$: The surface undergoes instability at a certain time t_C.

is always positive. It follows that the angle deformation is positive near the onset of instability. The $\varepsilon(t)$ obtained in this way is shown in Fig. 3. The corresponding deformation of the surface is smoothly concave in the region of $0<r<a$. This implies that the fluid surface is a cusp. It follows that the fluid changes from the Taylor cone to a cusp as the applied voltage V increases up to the breakdown voltage V_C.

As seen in Table 1, V_C is much lower than V_T, at the apex. This reduction is due to protrusion around the apex. These values of V_C are found in-reasonable agreement with experiments [7, 19-21]. As expected, V_C increases with increasing r. In the work of Kingham *et al.* [11], they have introduced an protrusion to explain experimental values of V_C. However, they have not presented any physical ground on such elongation. In the current work, we have introduced a protrusion as a result of the inward deformation of the surface in the apex region. The deformation is a solution of a set of electrohydrodynamic equations satisfied by the electrified fluid surface. Thus the obtained shape is regarded as one of profiles of an electrified fluid observed during experiment. This implies that the current work is a more exact treatment to explain the mechanism of operation of liquid metal ion sources than earlier works.

4. Conclusions

The realistic conical model of a conducting fluid has been presented to describe the electrohydrodynamic properties of liquid metal ion sources. In the current work, we introduced a protrusion h which is half the parametric value a, where a is defined such that there is no change in shape for $r>a$. We take the angular deformation $\zeta=(r/a)^s$ for $r<a$ and $(a/r)\varepsilon$ for $r>a$, where $0<s\leq 0.2$. This form of ζ satisfies the condition that $r\zeta$ is finite as r approaches to infinity. By considering deformation from the Taylor cone as the first-order correction to the surface, we have obtained the r- and h-dependent critical voltage, $V_C(r, h)$, which is needed for the onset of instability of the fluid, i.e. ion emission from the liquid surface. Thus the obtained V_C explains the local instability, which can not be explained by any static analysis. At the apex, V_C is in good agreement with experimental values. The form of ζ obtained in the current work represents a cusp near the onset of ion emission.

References

1. Lord Rayleigh, *Phil. Mag.* **14**, 184 (1882).
2. J. Zeleny, *Proc. Cambridge Phil. Soc.* **18**, 71 (1915).
3. D. S. Swatik and C. D. Hendricks, *AIAA J.* **6**, 1596 (1968).
4. S. Chandrasekhar, *Hydrodynamic and Hydromagnetic Stability* (Dover, New York, 1981).
5. J. R. Melcher, *Continuum Electromechanics* (MIT press, Cambridge, 1981).
6. J. F. Mahoney, A. Y. Yahiku, H. L. Daley, R. D. Moore and J. Perel, *J. Appl. Phys.* **40**, 5101 (1969).
7. R. Gomer, *Appl. Phys.* **19**, 365 (1979).
8. R. Clampitt and D. K. Jefries, *Nucl. Instr. Methods* **149**, 739 (1978).
9. G. I. Taylor, *Proc. Roy. Soc.(London) A280*, 383 (1964).
10. M. D. Gabovich, *Sov. Phys. Usp.* **26**, 447 (1983).
11. D. R. Kingham and L. W. Swanson, *Appl. Phys.* **A34**, 123 (1984).
12. D. L. Barr, W. L. Brown and D. J. Thompson, *J. Phys.(Paris)* **47**, C2-87 (1986).
13. V. V. Bladirov and V. N. Gorshkov, *Appl. Phys.* **A46**, 131 (1989).
14. S. Grossman and A. Muller, *Z. Phys.* **B57**, 161 (1981).
15. M. S. Chung N. M. Miskovsky, P. H. Cutler, T. E. Feuchtwang and E. Kazes, *J. Vac. Sci. Tchnol.* **B5**, 1628 (1987).
16. M. S. Chung, P. H. Cutler and N. M. Miskovsky, *J. Appl. Phys.* **66**, 6065 (1989).
17. M. S. Chung, P. H. Cutler, J. He and N. M. Miskovsky, *Surf. Sci.* **246**, 118 (1991).
18. Centre National d'Etudes de Telecommunications, *Tables Numeriques des Fonctions Associees de Legendre*, (Editions de La Revue d'Optique, Paris, 1959).
19. G. Benassayag, P. Sudrau and B. Jouffrey, *Ultramicoscopy* **16**, 1 (1985).
20. C. Zheng and T. Linsu, *J. Vac. Sci. Technol.* **B7**, 1813 (1989).
21. A. Wagner, *Appl. Phys. Lett.* **40**, 440 (1982).